CORA Cork Open Research Archive
Cartlann Taighde Oscailte Chorcaí

Title	A microbiota-informed pipeline for in vitro characterisation of insulinotropic properties of dairy fermentates using static EndoC-βH1 and dynamic microfluidic models
Authors	Garcia-Gutierrez, Enriqueta;Ponsero, Alise J.;Calero, Víctor;Slattery, Helen;Gonçalves, Catarina;Marroquí, Laura;Cotter, Paul D.
Publication date	2026-08-03
Original Citation	Garcia-Gutierrez, E., Ponsero, A. J., Calero, V., Slattery, H., Gonçalves, C., Marroquí, L. and Cotter, P. D. (2026) 'A microbiota-informed pipeline for in vitro characterisation of insulinotropic properties of dairy fermentates using static EndoC-βH1 and dynamic microfluidic models', Food Research International, 120207 (12pp). https://doi.org/10.1016/j.foodres.2026.120207
Type of publication	Article (peer-reviewed)
Link to publisher's version	10.1016/j.foodres.2026.120207
Rights	© 2026, the Author(s). Published by Elsevier Ltd. This is an open access article under the CC BY license (http://creativecommons.org/licenses/by/4.0/). - https://creativecommons.org/licenses/by/4.0/
Download date	2026-11-16 05:57:07
Item downloaded from	https://hdl.handle.net/10468/19235

UCC
University College Cork, Ireland
Coláiste na hOllscoile Corcaigh

Food Research International 242 (2026) 120207



Contents lists available at ScienceDirect

Food Research International

journal homepage: www.elsevier.com/locate/foodres





A microbiota-informed pipeline for in vitro characterisation of insulinotropic properties of dairy fermentates using static EndoC-βH1 and dynamic microfluidic models

Enriqueta Garcia-Gutierrez [a,b,c,d], Alise J. Ponsero [e], Víctor Calero [f,g], Helen Slattery [a], Catarina Gonçalves [g], Laura Marroquí [h,i], Paul D. Cotter [a,b,c,*]

[a] Teagasc Food Research Centre, Moorepark, Fermoy, P61 C996 Co, Cork, Ireland.
[b] APC Microbiome Ireland, University College Cork, T12 YN60 Co., Cork, Ireland.
[c] VistaMilk SFI Research Centre, Moorepark, Fermoy, P61 C996 Co., Cork, Ireland
[d] Department of Agronomic Engineering, Technical University of Cartagena, member of European University of Technology EUT+, Paseo Alfonso XIII, 48, 30203 Cartagena, Spain
[e] Core Bioinformatics, Quadram Institute Bioscience, Norwich, Norfolk, United Kingdom
[f] Applied Physics Department, University of Oviedo, Asturias, Spain
[g] Iberian Nanotechnology Laboratory, Braga, Portugal
[h] Instituto de Investigación, Desarrollo e Innovación en Biotecnología Sanitaria de Elche (IDiBE), Universidad Miguel Hernández de Elche, 03202, Elche, Spain
[i] CIBER de Diabetes y Enfermedades Metabólicas Asociadas (CIBERDEM), Instituto de Salud Carlos III, 28029, Madrid, Spain

ARTICLE INFO

Keywords:
Beta cells
SCFA
Gut microbiota
Dairy fermentates
Diabetes
Insulin secretion
Dynamic secretion
Microfluidics

ABSTRACT

Diabetes mellitus (DM), which encompasses Type 1, Type 2 and gestational diabetes, affects approximately 537 million adults, with prevalence continuing to rise. In addition to pregnancy, factors such as dietary choices, lifestyle and infections can lead to the development of DM. Given the increasing prevalence of DM, it is necessary to continue to identify approaches to control the release of insulin. Emerging evidence indicates that the gut microbiota plays a central role in mediating the metabolic effects of diet on the host, including the regulation of insulin secretion. Dietary interventions have been proven to be successful in this regard, but identifying foods and food components that influence insulin secretion is challenging due to the complexity of diet-microbiota-host interactions and the lack of fast and standardised screening tools. We have developed a novel screening framework based on the β-cell insulin response, using the human cell line EndoC-βH1 to assess candidate foods and ingredients with insulinotropic properties. As an initial proof-of-concept, we applied the framework to food ingredients, i.e., dairy-derived fermentates, which had first undergone simulated digestion followed by addition to an ex vivo colon model, allowing us to mimic the metabolic transformations taking place in the human gut. The processed colonic fermentation supernatants were then evaluated using a static and microfluidic platform, respectively, to capture dynamic insulin release profiles. Distinct fermentate compositions were associated with varying levels of insulin secretion. Our results suggest that this framework could be applied broadly to screen foods and food components for insulinotropic potential, providing an affordable approach for the development for anti-diabetic dietary applications.

1. Introduction

Diabetes mellitus (DM) is a significant global health issue, with a continuously increasing prevalence, estimated to reach 643 million adults affected by 2030 (Sun et al., 2022). Approximately 5–10% of people living with diabetes suffer from Type 1 Diabetes (T1D), an autoimmune condition where pancreatic β cells producing insulin are targeted by the immune system (Katsarou et al., 2017; Magliano and Boyko, 2021). The other 90–95% live with Type 2 Diabetes (T2D), which is characterised by the insufficiency in insulin production and/or the development of certain level of resistance to that insulin in tissue (Chatterjee et al., 2017). Gestational Diabetes Mellitus (GDM) reports a

* Corresponding author at: Teagasc Food Research Centre, Moorepark, Fermoy, P61 C996 Co., Cork, Ireland
E-mail addresses: enriqueta.garcia@upct.es (E. Garcia-Gutierrez), paul.cotter@teagasc.ie (P.D. Cotter).

https://doi.org/10.1016/j.foodres.2026.120207
Received 13 May 2026; Received in revised form 23 July 2026; Accepted 28 July 2026
Available online 31 July 2026
0963-9969/© 2026 The Author(s). Published by Elsevier Ltd. This is an open access article under the CC BY license (http://creativecommons.org/licenses/by/4.0/).

variable percentage of prevalence depending on countries, affecting approximately 14% of pregnancies, ranging from 7 to 25% depending on diagnostic criteria and population studied (Magliano and Boyko, 2021; McIntyre et al., 2019). However, GMD is considered a transient condition and is not included in the prevalence percentages of other chronic forms of diabetes.

DM causes are varied and depend on the type. For T1D there are genetic factors that can be triggered by environmental factors, such as viral infections (Burke et al., 2020; Knip et al., 2005; Nekoua et al., 2022), while, for T2D, lifestyle choices, such as diet, play a more important role (Martinez et al., 2017). GDM, on the other hand, seems to be linked to levels of inflammation (Mirghani Dirar and Doupis, 2017). However, other factors have been associated with the development of DM, such as low income and other socioeconomic factors that result in individuals not having access to food of sufficient nutritional quality (O'Hearn et al., 2023). DM is also, in turn, linked with a variety of diabetes-related complications, such as cardiovascular diseases, lower-extremity complications or diabetes retinopathy, increasing the personal, social and economic burden of the condition (Dal Canto et al., 2020).

The link between DM and diet has been extensively studied. However, as a consequence of the considerable advances in the capacity to study the gut microbiota, some new insights have been provided, offering potential intervention opportunities. More specifically, there is growing evidence of connections between gut microbiota dysbiosis and suboptimal health conditions, including DM among others (Martinez et al., 2017; Tai et al., 2015). As a result, different strategies for gut microbiota modulation have been proposed, including clinical interventions (such as Faecal Microbiota Transplant (FMT)) or more targeted approaches, including the use of specific bacteriophages (Lijuan et al., 2023; Ye et al., 2024).

Dietary interventions have been highlighted as a way to modulate a sub-optimal gut microbiota and promote health-associated biomarkers. Fermented foods and fermentates (powdered ingredients generated through fermentation) are attracting attention as foods/ingredients that could help and/or alleviate conditions associated with an altered gut microbiota, including diabetes (Awwad et al., 2022; Sivamaruthi et al., 2018).

Here, we develop a pipeline to screen food components according to their insulinotropic properties, in a manner that considers impacts facilitated by the gut microbiota. To this end, we digested six fermentates following the INFOGEST protocol, an in vitro model of upper gastrointestinal digestion, and investigated their impact on the gut microbiota, the taxonomic changes as well as short chain fatty acid (SCFA) profile, in an ex vivo model of the human distal colon. We further evaluated the effect of this colonic material (in the form of cell free supernatants) on the insulin secretion response in a static in vitro model using EndoC-βH1, a cell line validated for studying β-cell pancreatic response in humans. Additionally, we used a microfluidics approach, which facilitates a dynamic assessment of secretion, using mouse pancreatic islets to investigate the profiles of insulin release with time. To the best of our knowledge, this represents the first proof-of-concept application exploring the impact of dairy fermentates, modulated by gut microbiota activity, on pancreatic function using both a static human β-cell model (EndoC-βH1) and a dynamic system. This strategy is designed to evaluate the feasibility of integrating microbiota-derived metabolites with β-cell functional assays, and to lay the groundwork for future, more comprehensive studies.

2. Methods

2.1. In vitro digestion of the dairy fermentates

2.1.1. Dairy fermentate composition and selection

Six dairy fermentates were provided by Carbery Ltd. (Ballineen, West Cork, Ireland) as representatives of the same product category (dairy-derived fermentates) but with different macronutrient compositions, spanning from high-lactose/moderate-protein to high-protein/low-lactose profiles. This would allow to assess the discriminatory capacity of the pipeline across a diverse set of ingredients within the same food category (Table 1).

2.1.2. INFOGEST in vitro digestion

A small portion (5 g) of each dairy fermentate was subjected to simulated gastrointestinal digestion following the standardised INFOGEST static protocol (Brodkorb et al., 2019). Briefly, the oral phase was performed by mixing the sample with 4 ml of Simulated Salivary Fluid (SSF), followed by addition of 0.3 M $CaCl_2(H_2O)_2$ and distilled water to bring the volume to 10 ml. The gastric phase was performed by mixing 10 ml of the oral sample with 7.5 ml of Simulated Gastric Fluid (SGF) and 1.6 ml of porcine pepsin stock solution (2500 U/ml; Sigma Aldrich, Ireland), with 5 μl of 0.3 M $CaCl_2(H_2O)_2$ added and pH adjusted to 3 using 1 M HCl. The mixture was incubated at 37 °C for 2 h with shaking. The intestinal phase was initiated by adjusting the pH to 7 using 1 M NaOH, followed by mixing 20 ml of the gastric chyme with 11 ml of Simulated Intestinal Fluid (SIF), 5 ml of pancreatin solution (800 U/ml; Sigma Aldrich, Ireland), 2.5 ml of fresh bile solution (1.25 g dried bile resuspended in 12.5 ml SIF; Sigma Aldrich, Ireland), and 40 μl of 0.3 M $CaCl_2(H_2O)_2$. The intestinal phase was incubated at 37 °C for 2 h with shaking. Digestion was terminated by heating at 60 °C for 20 min to inactivate enzymes, followed by centrifugation at 4000 rpm for 5 min, pH adjustment to 7, and sterile filtration of the supernatant.

2.2. Ex vivo distal colon model studies

2.2.1. Preparation of a faecal standard

The faecal slurry was prepared as described previously (O'Donnell et al., 2016). The Clinical Research Ethics Committee of the Cork Teaching Hospitals, UCC, approved the study (ECM 4 (mm) 09/03/2021) and faecal samples from healthy donors without antibiotic treatment in the previous six months were collected after written consent. Samples were kept at 4 °C for 1–2 h, and a mixture of 200 g in total were processed in an anaerobic chamber (5% CO_2, 10% H_2 and 85% N_2) by mixing them with 200 ml saline buffer containing 0.05% (*w/v*) cysteine hydrochloride in a Circulator 400 stomacher bag (Seward, UK). The mixture was homogenised, centrifuged (4000 ×*g*, 25 min) and resuspended in PBS. Sterile glycerol was added to a final concentration of 25%, aliquoted and stored at −80 °C.

2.2.2. Ex vivo distal colon model experiments

A faecal slurry aliquot was defrosted diluted 1:10 in faecal fermentation medium (Fooks and Gibson, 2003). The six digested dairy fermentates were added to designated wells of the micro-Matrix plate, in duplicates, at a concentration of 1 and 5% *w/v* to a final volume of 6 ml in the faecal slurry diluted 1:10 in faecal fermentation medium (Fooks and Gibson, 2003). Control wells containing the diluted faecal slurry were also included. A 1 ml aliquot was removed from each well at time 0 (T0), reducing the fermentation volume to 5 ml per well. The fermentations were conducted for 24 h at 37 °C and shaking at 300 rpm, with medium pH adjusted and maintained at 6.8 in a micro-Matrix

Table 1
Composition of the six dairy fermentates.

Fermentate number	**Protein (%)**	**Moisture (%)**	**Fat (%)**	**Lactose (%)**	**Not disclosed (%)**
1	56	5	5	30	4
2	80	5	6	3	6
3	80	5	5.5	3	6.5
4	90	5	1.3	0.8	2.9
5	90	4.5	0.5	<0.5	5
6	35	5.5	0.6	0	58.9

fermenter (Applikon Biotechnology). Aliquots of 1 ml were collected from each well and kept at -80 °C for further analyses.

2.3. Gut microbiome characterisation

2.3.1. DNA extraction

The 1 ml aliquots had their gDNA extracted using QIAmp PowerFecal ProDNA kit (Qiagen, UK), following manufacturer's instructions. Briefly, the centrifuged samples (4000 rpm, 10 min) were resuspended in lysis buffer and the extractions were performed according to the manufacturer's instructions. DNA was quantified using the Qubit 2.0 Fluorometer (Life Technologies, USA) and the purity checked using the NanoDrop 1000 (ThermoFisher Scientific, Ireland).

2.3.2. Sequencing and bioinformatics analyses

DNA was prepared according to the Nextera XT DNA library preparation guide from Illumina and sequenced on an Illumina NextSeq (Teagasc, Moorepark Sequencing Facility) using a protocol for shallow shotgun, as it reduces technical variations (La Reau et al., 2023), using 2 × 150 bp paired-end kit on the Illumina NextSeq Platform (Teagasc, Moorepark Sequencing Facility), with base-calling using bcl-convert (v3.8.4).

Raw sequencing reads were processed through a multi-step quality control and taxonomic profiling pipeline. Host reads were removed using Hostile (v2.0.0) (Constantinides et al., 2023) with the human-t2t-hla reference database and Bowtie2 (Langmead and Salzberg, 2012) as the alignment engine. Across the 26 experimental samples, the proportion of human-mapping reads was negligible, ranging from 0.001% to 0.003%, confirming minimal host DNA contamination in the faecal fermentation matrix. The two negative sequencing controls yielded very low read counts (1314 and 920 reads respectively) and were entirely unclassified upon taxonomic profiling, indicating no detectable microbial contamination of the sequencing run. Following host removal, reads were quality-trimmed using Trim Galore (v0.6.10) (Krueger, 2015). Taxonomic profiling was performed using MetaPhlAn4 (Blanco-Míguez et al., 2023) (v4.1.1; database mpa_vJan25_CHOCOPhlAnSGB_202503). Experimental samples had a mean sequencing depth of approximately 3.37 million reads (range: 850,916–8,456,008) after host removal. The proportion of unclassified reads across experimental samples ranged from 0% to 12.3%, with all samples showing high classification rates consistent with a human gut-derived microbial community.

Consistency between technical replicates were assessed by Spearman rank correlation of relative abundances at species and family level across all condition-concentration pairs with paired replicates (supplemental Fig. 1). Correlations were generally high across colonic fermentate conditions, with species-level rho ranging from 0.691 to 0.951 and family-level rho from 0.865 to 0.976. However, the T24 control condition showed notably lower inter-replicate agreement at both species (rho = 0.675) and family level (rho = 0.644), driven by the high variability in the relative abundance of *Escherichia coli* between replicates (44.5% ± 17.2%). Consequently, the T24 control was not used as the reference condition for differential abundance analyses. Instead, the T0 community, which showed high replicate consistency (species rho = 0.951, family rho = 0.976), was retained as the baseline reference.

Alpha diversity was assessed using observed species richness (number of species with relative abundance >0), Shannon entropy, and Pielou evenness using the microbiome R package v1.28.0. Given the limited number of replicates per group (n = 1–2), results are reported descriptively. One sample (Ferm4 5% R2) was excluded from all alpha diversity analyses due to insufficient sequencing depth (850,916 reads), representing a ~ 10-fold imbalance relative to its paired replicate (8,456,008 reads) that would artificially inflate observed richness comparisons.

2.3.3. Organic acids measurements

Aliquots were defrosted and filter sterilised using 0.2 μm-pore-size syringe filters (Whatman International Ltd., UK) and 300 μl injected into Chromacol vials (Fisher Scientific, UK). Concentrations of formic, acetic, lactic, citric, propionic and butyric acid were quantified by HPLC using a Perkin-Elmer Flexar HPLC system coupled with refractive index and photo diode array detectors for 210, 280 and 325 nm wavelengths (PerkinElmer Inc., USA). Analyses were conducted using an Rezex™ ROA-Organic Acid H^+ (8%) LC column coupled with a refractive index detector with a sensitivity set at 512. The column was set at 60 °C and the eluent 0.005 N H_2SO_4 was run at 0.6 ml/min. A standard curve was constructed using reference concentrations at concentrations from 10 μg/ml to 100 μg/ml formic, acetic, lactic, citric, propionic and butyric acids (all from Sigma Aldrich). Results are presented descriptively due to the limited number of replicates. Concentration values were converted from μg/ml to mM using the molecular weights of each acid.

2.3.4. Sugars measurements

Samples were separated and quantified for lactose, glucose and galactose using an Aminex HPX 87C fixed ion resin column. The column was set at 60 °C and the eluent 0.009 N H_2SO_4 was run at 0.5 ml/min. The sugars were detected using a refractive index detector with a sensitivity set at 512, an internal temperature set at 35 °C and a positive polarity. Calibration curves for the 3 sugars were generated using different concentrations 10, 20, 50 and 100 μg/ml giving a linear response.

2.4. Static secretion in EndoC-βH1 cell line

The human EndoC-βH1 β-cell line (research resource identifier (RRID):CVCL_L909, Univercell-Biosolutions, France) was grown attached to Matrigel/fibronectin-coated plates (Ravassard et al., 2011). Cells were cultured in DMEM, containing 5.6 mM glucose, 10 mM nicotinamide, 5.5 μg/ml transferrin, 50 μM 2-mercaptoethanol, 6.7 ng/ml selenite, 2% BSA fatty acid free, 100 U/ml penicillin, and 100 μg/ml streptomycin.

Each well was incubated with 200 ul of βKrebs® (Human Cell Design, GSIS buffer) supplemented with 0.1% fatty acid free Bovine Serum Albumin Fraction V (Roche) at 37 °C. After 2 h, the buffer was removed and substituted with 150 ul of the colonic fermentation supernatants (CFS) diluted 1:25 in the βKrebs® + 0.1% BSA buffer. To test the effect of pure propionic and butyric acids, EndoC-βH1 cells were incubated at increasing physiological and supraphysiological concentrations of both organic acids (10, 18, 25 and 100 mM) in the same way as the CFS. Controls were low glucose (βKrebs® + 0.1% BSA+ 0 mM glucose) and 20 mM glucose (βKrebs® + 0.1% BSA with (D (+) glucose anhydrous for analyses (Applichem)). The cells were incubated at 37 °C for 1 h and 75 ul of buffer were recovered and kept in ice, centrifuged at 700 xg at 4 °C for 5 min and 50 ul of them were stored at −20 °C for conducting the ELISA, using the 10–1113-01 Mercodia Insulin ELISA kit (Mercodia) following manufacturer's recommendations.

Pearson correlation analysis was performed to investigate the relationships between fermentate compositional variables (protein, moisture, fat and lactose content, expressed as %), organic acid concentrations measured in colonic fermentation supernatants (formic, acetic, propionic, lactic, butyric and citric acid), and mean insulin secretion in EndoC-βH1 cells averaged across three independent experiments. Pearson correlation coefficients and associated p-values were calculated using the scipy.stats.pearsonr function in Python (v3.12). Statistical significance was set at $p < 0.05$ (n = 22). Only significant correlations are displayed in the correlation matrix; non-significant pairs are shown in grey. The correlation matrix was visualised using matplotlib (v3.10.8).

2.5. Dynamic insulin secretion profiling of colonic fermentation supernatants using a microfluidics perfusion system

2.5.1. Design and fabrication of microfluidic devices

The microfluidic devices were fabricated on polymethyl

methacrylate (PMMA) using a laser cutter in a layer-by-layer approach. The devices consisted of two 2-mm wide 1-mm tall channels (an inlet and an outlet) that converged in a 5-mm diameter central chamber (Fig. 1A and B). In the central chamber both channels were separated by a microporous polyester (PET) 11-µm thick membrane with 1-µm pores (2000 M12/620 M103/R3ipCELLCULTURE Track-Etched Membrane, Sigma-Aldrich, Portugal), so that the islets could rest on top of the membrane and the secretions could be collected via the outlet channel in a continuous flow. The final device was assembled by adhering the bottom and top channels with the membrane in between using double-sided tape (3 M155980-ND12SQ-12-467MP, 3 M™) (Fig. 1C). The fluid flow rate was controlled using a Multi-Phaser™ NE-1600 syringe pump connected to the input channel. Buffers and samples were placed in 1 ml syringes and the flow circulated at 50 µl/min. The devices were placed on a hot plate regulated at 37 °C to maintain the temperature of the islets and allow the secretion of insulin (Fig. 1D).

2.5.2. Mice pancreatic islets isolation

Adult male mice (12–14-weeks-old), which were kept under standard housing conditions (12 h light/dark cycle, food ad libitum), were sacrificed and pancreatic islets were isolated as described before (Nadal and Soria, 1997). After the isolation, islets were kept at 37 °C in a humidified atmosphere of 95% O_2 and 5% CO_2 until their use within the same day. Experimental procedures were performed according to the Spanish Royal Decree 1201/2005 and the European Community Council directive 2010/63/EU. The ethical committee of Miguel Hernandez University reviewed and approved the methods used herein (approvals ID: UMH.DF.LME.01.20 and UMH.IDI.LME.240119).

2.5.3. Dynamic insulin secretion

Krebs-Ringer buffer containing 115 mM NaCl, 5 mM KCl, 1 mM $MgCl_2$, 1 mM $CaCl_2$, 24 mM $NaHCO_3$, 10 mM HEPES, pH 7.4, and 0.1% BSA, was supplemented with 0 and 20 mM of glucose and left opened to re-equilibrate in an incubator at 37 °C. Islets were selected attending to morphological criteria, with similar sizes and colour, placed in starving (Krebs buffer supplemented with 0 mM glucose) for 1 h and moved with a Pasteur pipette into the chambers of the devices, 2 per chamber, along with filling the chamber with Krebs buffer to avoid desiccation. Krebs buffer 0 mM was previously run over the system to wash potential particulates.

The islets were exposed to buffers following pattern: 5 min 0 mM glucose; 10 min of the colonic fermentation supernatant diluted 1:25; 5 min 0 mM glucose and 10 min challenge of 20 mM glucose; which flowed at 50 µll/min. An aliquot was collected every 2 min, immediately kept in ice and stored at −20 °C for conducting the ELISA, using the 10–1250-10 Mercodia Insulin ELISA kit following manufacturer's recommendations.

2.5.4. Area under the curve (AUC) calculation and statistical analysis

Insulin secretion was quantified by calculating the area under the curve (AUC) using the trapezoidal rule (Le Floch et al., 1990), applied to the colonic fermentate supernatant treatment phase (t = 6–16 min). All three experimental groups comprised n = 3 independent biological replicates. To control for variability in islet quality between independent preparations, the colonic fermentate supernatant-phase AUC values were normalised to the AUC of the 20 mM glucose response (t = 20–30 min) for the corresponding replicate and expressed as a percentage (normalised AUC = fermentate AUC / glucose AUC × 100). Differences between groups were assessed by one-way analysis of variance (ANOVA). Post-hoc pairwise comparisons were performed using Tukey's honestly significant difference (HSD) test. Statistical analyses were performed using GraphPad Prism 8. Results are expressed as mean ± standard deviation (SD) and statistical significance was defined as $p < 0.05$.

3. Results

3.1. Dairy fermentates modulate gut microbial community structure, diversity and metabolite production during colonic fermentation

3.1.1. Effects at community level

Dairy fermentates were subjected to in vitro digestion and then added to an ex vivo model distal colon microbiota to assess the impact on the associated microbial community. At T0, the microbial community was characteristic of a healthy human gut microbiome, dominated at the family level by Lachnospiraceae (35.0% ± 0.3%), Oscillospiraceae (16.2% ± 0.2%), Bacteroidaceae (12.9% ± 0.8%), and Bifidobacteriaceae (12.4% ± 1.1%) (Fig. 2A). At the species level, the most abundant taxa were *Bacteroides uniformis* (6.83% ± 0.21%), *Bifidobacterium adolescentis* (6.27% ± 0.50%), *Faecalibacterium prausnitzii* (5.75% ±

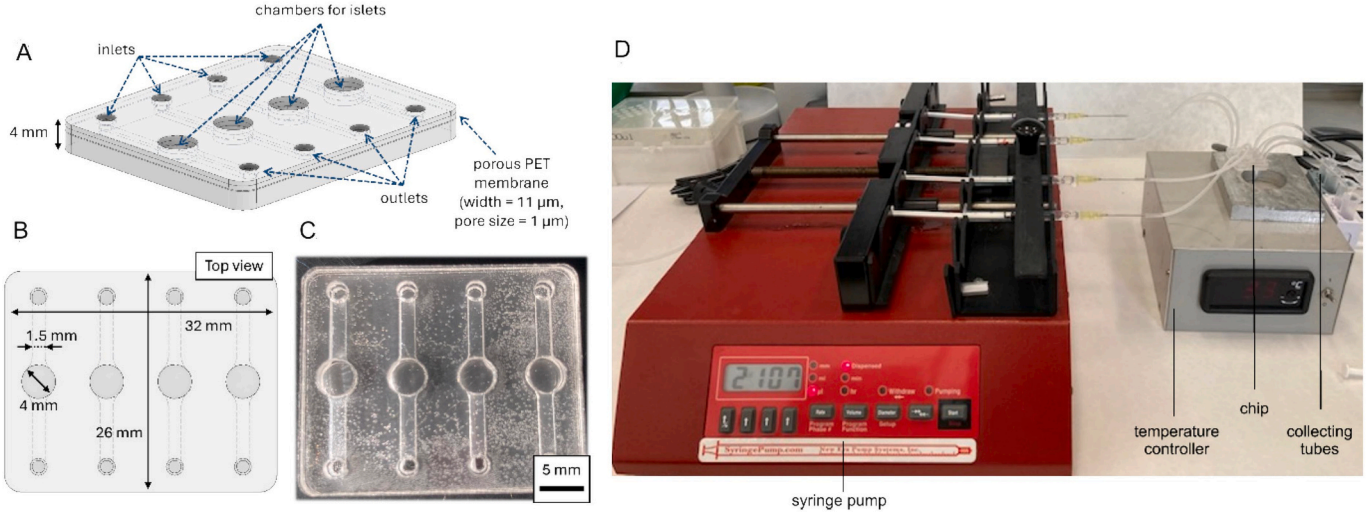
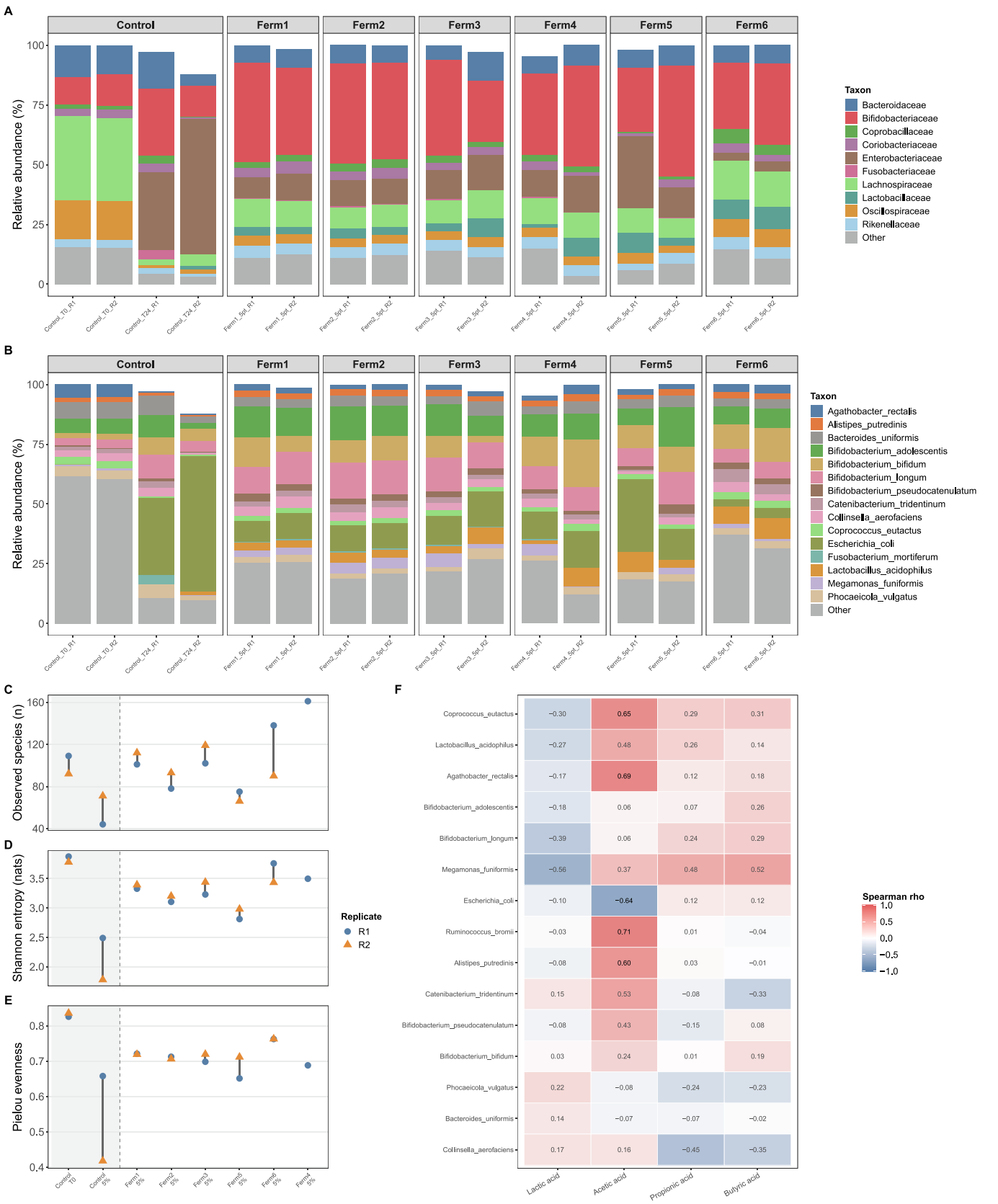


Fig. 1. Microfluidic chip design and perfusion system used for dynamic insulin secretion measurements. (A) Schematic representation of the microfluidic chip showing the 3D design and (B) top view with dimensions. The chip contains four independent islet chambers (4 mm diameter) connected by microchannels (1.5 mm width), with an overall chip footprint of 32 × 26 mm. (C) Photograph of the fabricated PMMA chip (scale bar = 5 mm). (D) Photograph of the perfusion system, comprising a syringe pump delivering solutions at a controlled flow rate, a temperature controller maintaining physiological conditions, the microfluidic chip, and collecting tubes for fraction collection for subsequent insulin quantification.



(caption on next page)

Fig. 2. Gut microbial community composition, diversity, and taxa-SCFA associations following 24 h in vitro fermentation with dairy fermentates at 5% concentration. All panels include the unfed control at T0 (start of fermentation, Control T0) and T24 (24 h fermentation without fermentate, Control T24) alongside fermentate-treated conditions (Ferm1–Ferm6 at 5% *w/v*). (A) Family-level and (B) species-level relative abundance profiles shown as stacked bar charts. Individual replicates are shown. Taxa not among the top 10 (family) or top 15 (species) most abundant across all samples are grouped as "Other" (grey). Colours are consistent between panels A and B. (C, D, E) Alpha diversity across conditions shown as lollipop plots for three metrics: observed species richness (number of species with relative abundance >0), Shannon entropy (nats), and Pielou evenness. Each lollipop represents one condition; individual replicates are shown as circles (R1, blue) and triangles (R2, orange), connected by a vertical segment where both replicates are available. The shaded grey area indicates control groups. One sample (Ferm4 5% R2) was excluded due to low sequencing depth (see Methods). (F) Spearman rank correlation heatmap between the 15 most abundant species and four key short-chain fatty acids (acetic, propionic, butyric, and lactic acid) across 5% fermentate samples and Control T24 ($n = 13$; $n = 12$ for lactic acid). Colour intensity reflects the magnitude and direction of correlation (red: positive, blue: negative). Values with $|rho| > 0.6$ are shown in bold. Results are descriptive; no significance threshold was applied given sample size. (For interpretation of the references to colour in this figure legend, the reader is referred to the web version of this article).

0.13%), *Ruminococcus bromii* (5.46% ± 0.54%), and *Agathobacter rectalis* (5.35% ± 0.15%) (Fig. 2B). Following 24 h, the control condition showed a marked shift in community composition characterised by a substantial bloom of *Escherichia coli* (44.5% ± 17.2%), corresponding to a dominance of Enterobacteriaceae at family level. Bifidobacteriaceae remained the second most abundant family (20.5% ± 10.7%), while Lachnospiraceae declined sharply compared to T0 (3.67% ± 1.53%). In contrast, samples supplemented with dairy fermentates at 5% concentration showed a substantially attenuated *E. coli* bloom (12.1% ± 6.79%) and a pronounced enrichment of Bifidobacteriaceae (36.4% ± 6.89%), driven by increases in the relative abundance of *B. adolescentis* (11.1% ± 3.08%), *Bifidobacterium longum* (11.0% ± 3.13%), and *Bifidobacterium bifidum* (10.6% ± 4.11%). *Lactobacillus acidophilus* was also enriched (5.08% ± 2.53%), and Lachnospiraceae were better maintained (11.1% ± 2.40%) relative to the unsupplemented control. Following the addition of fermentates at 1% fermentate concentration, community composition at T24 closely resembled the unfed control rather than the 5% fermentate condition, highlighting that the modulatory effect of the dairy fermentates on the gut microbial community is concentration-dependent (Supplemental Fig. 2).

3.1.2. Effects in alpha diversity

In terms of alpha diversity, the inoculum community showed high diversity and evenness at T0, with 100 ± 12 observed species, a Shannon entropy of 3.83 ± 0.07, and a Pielou evenness of 0.831 ± 0.007. Following 24 h without fermentate, the unfed control showed a marked reduction across all three metrics (57.5 ± 19.1 observed species, Shannon 2.13 ± 0.50, Pielou 0.538 ± 0.17), consistent with the *E. coli* bloom observed in the composition analysis and the high between-replicate variability noted previously.

At 5% fermentate concentration, alpha diversity was substantially preserved relative to the unfed T24 control across all fermentate conditions. Observed species richness ranged from 70.5 ± 6.4 (Ferm5) to 161 (Ferm4, single replicate), Shannon entropy from 2.90 ± 0.12 (Ferm5) to 3.60 ± 0.23 (Ferm6), and Pielou evenness from 0.681 ± 0.04 (Ferm5) to 0.763 ± 0.00 (Ferm6) (Fig. 2C). The majority of fermentate conditions at 5% approached or matched T0 diversity levels across all three metrics, indicating that the fermentates broadly supported maintenance of community diversity during in vitro fermentation. Notably, Ferm5 consistently showed the lowest diversity values at 5% concentration across all three metrics, which may relate to its distinct macronutrient composition: the highest protein content (90%) combined with near-absent lactose (<0.5%) and the lowest fat content (0.5%) among all fermentates tested (Table 1). Conversely, Ferm6 showed the highest Shannon entropy and Pielou evenness at 5%, and is compositionally distinct in having the highest proportion of undisclosed components (~58.9%) alongside the lowest protein content (35%) among the fermentates.

3.1.3. Taxa-organic acid associations

To explore the relationship between community composition and fermentation metabolite production, Spearman rank correlations were computed between the relative abundance of the 15 most abundant species and four key organic acids (acetic, propionic, butyric, and lactic acid) across the 5% fermentate samples and the T24 control ($n = 13$ samples; $n = 12$ for lactic acid due to one missing value). Given the sample size, all results are reported descriptively without *p*-value thresholding (Fig. 2F).

Acetic acid showed the strongest and most consistent associations across taxa. *Ruminococcus bromii* (rho = 0.714), *Agathobacter rectalis* (rho = 0.687), *Coprococcus eutactus* (rho = 0.654), and *Alistipes putredinis* (rho = 0.604) are known commensal fermenters and were all positively associated with acetic acid concentrations. These taxa are characteristic of a diverse, healthy gut community and were among those most depleted in the unfed T24 control, consistent with their positive relationship with fermentate-associated acetic acid production. Conversely, *E. coli* showed a negative association with acetic acid (rho = −0.637), in line with its bloom under conditions where these commensal species are reduced. *Catenibacterium tridentinum* (rho = 0.527) and L. *acidophilus* (rho = 0.484) also showed modest positive associations with acetic acid.

Bifidobacterium species, despite their marked enrichment at 5% fermentate concentration, showed weak associations with all four organic acids measured ($|rho| \leq 0.385$ across all pairs), suggesting that the *Bifidobacterium* bloom does not strongly co-vary with the measured organic acid concentrations under these conditions, or that their metabolic contribution may be reflected in metabolites not measured here such as acetate via a different pathway or lactate.

Associations with propionic and butyric acid were generally weaker. *Collinsella aerofaciens* showed negative associations with both propionic (rho = −0.451) and butyric acid (rho = −0.346). Lactic acid associations were modest overall, with *B. longum* showing the strongest association (rho = −0.385) (Supplemental Fig. 4).

3.2. Colonic fermentation of dairy fermentates induces distinct organic acid profiles

Samples from the simulated ex vivo colonic experiments were analysed for major fermentation acids, including organic acids formic, acetic, propionic, lactic, butyric and citric (Fig. 3). In the control samples, all organic acids increased over time. However, addition of the fermentates resulted in different profiles. Citric acid did not show differences between the 1% and 5% concentrations of the fermentates, except for fermentate 6, which displayed higher levels of citric acid at 5%. Similarly, fermentates 1, 2, 3, 4 and 6 showed higher concentrations of acetic acid at 5%, except concentration 5, which declines at 5%. Formic and lactic acids showed a decrease in all fermentates at 5% concentrations. On the other hand, propionic and butyric showed the opposite trend and 5% concentrations showed a sharp increase for fermentates 3, 4 and 5 in comparison with the unfed blank sample at 24 h and their 1% counterparts, with moderate increases in the case of fermentates 1, 2 and 6. Glucose, lactose and galactose were not recovered after the ex vivo colonic samples.

3.3. Colonic fermentation supernatants stimulate insulin secretion in EndoC-βH1 cells in a concentration-dependent manner

Static insulin secretion was assessed in EndoC-βH1 cells following incubation with supernatants from the aforementioned ex vivo colonic

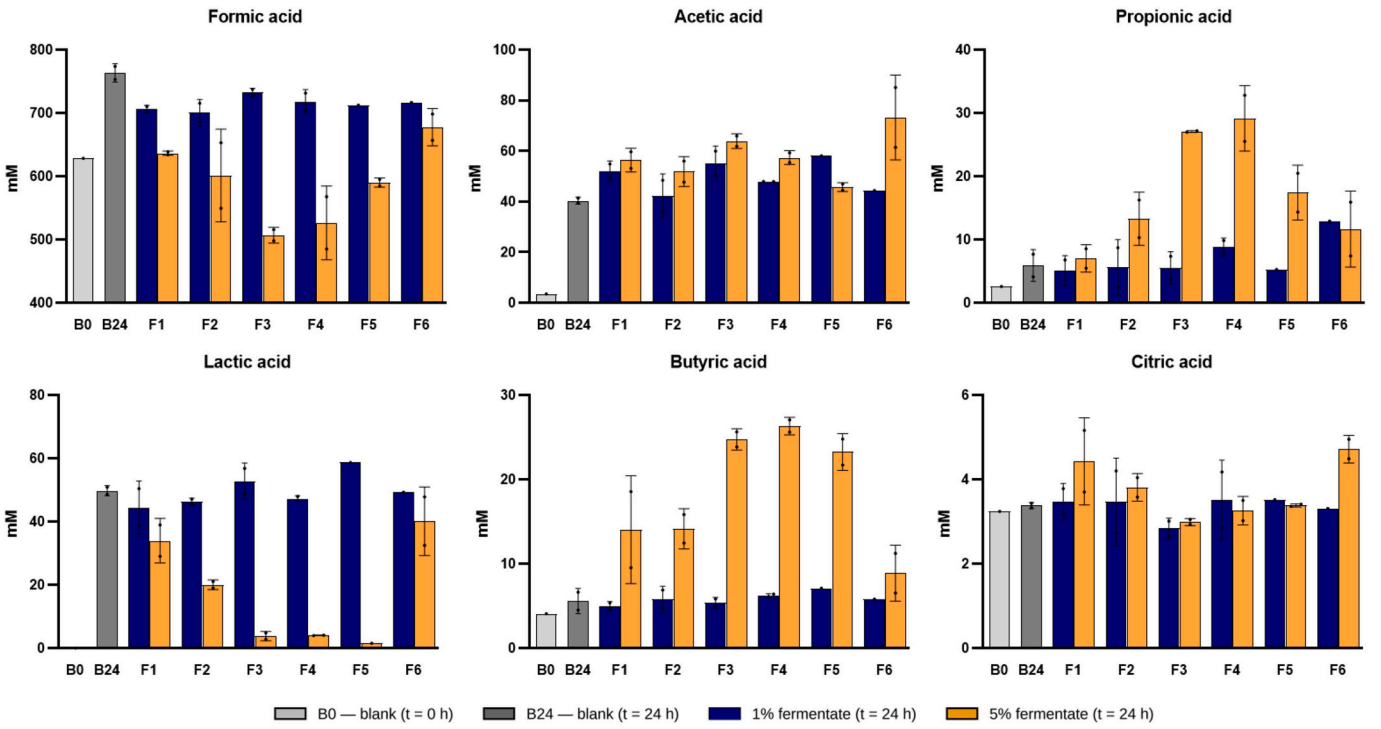


Fig. 3. Organic acid profiles of the ex vivo colonic fermentate supernatants derived from INFOGEST-digested dairy fermentates. Concentrations of formic, acetic, propionic, lactic, butyric and citric acids were measured by HPLC in colonic fermentation supernatants following 24 h incubation with digested dairy fermentates 1–6 at 1% (blue bars) and 5% (orange bars)(*w/v*) concentration. B0 and B24 correspond to uninoculated blanks at 0 and 24 h respectively. Bars represent mean ± SD; individual data points are shown. Concentration values were converted from μg/ml to mM using the molecular weights of each acid. (For interpretation of the references to colour in this figure legend, the reader is referred to the web version of this article).

experiments across three independent experiments (Fig. 4). In all three experiments, 20 mM glucose used as a positive control induced consistent insulin secretion, confirming the validity of the assay, while 0 mM glucose and the blank consistently showed the lowest secretion values, as expected. A concentration-dependent trend was observed across most CFS, with the 5% concentration generally inducing higher insulin secretion than the 1% concentration, particularly in CFS 1–5. CFS 6 showed the least pronounced concentration-dependent response across experiments. The absolute insulin secretion values differed substantially between the three independent experiments, which is consistent with the known variability in insulin secretory capacity between EndoC-βH1 cell passages. Due to this inter-experiment variability, and to confirm that the patterns of insulin secretion were consistent across independent experiments despite differences in absolute values, we performed a Pearson correlation analysis on the mean insulin secretion values for each condition across all experiment pairs (Supplementary Fig. 5), indicating that all pairwise correlations were statistically significant: Experiment 1 vs Experiment 2 ($r = 0.626$, $p = 0.030$), Experiment 1 vs Experiment 3 ($r = 0.856$, $p < 0.001$) and Experiment 2 vs Experiment 3 ($r = 0.885$, $p < 0.001$) for colonic fermentation supernatants response. These results indicate that while absolute insulin secretion values varied between cell passages, the ranking of induced insulin responses was reproducible across independent experiments, supporting the validity of the observed trends.

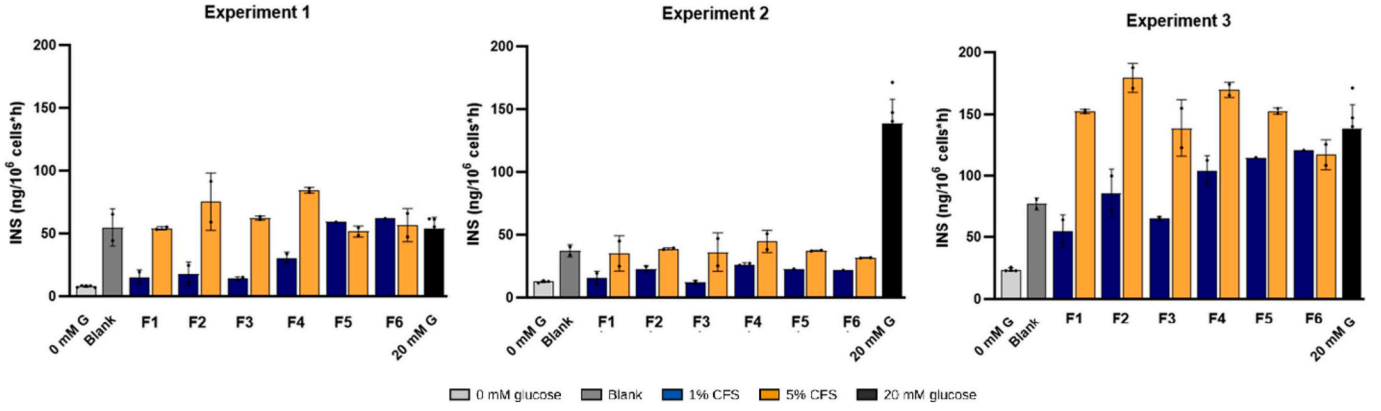


Fig. 4. Static insulin secretion in EndoC-βH1 cells in response to colonic fermentation supernatants derived from INFOGEST-digested dairy fermentates. A) Static insulin secretion in EndoC-βH1 cell line following 1 h static incubation with colonic fermentation supernatants (CFS) from dairy fermentates 1–6 at 1% and 5% (*w/v*). 0 mM glucose and 20 mM glucose were used as negative and positive controls respectively. The blank corresponds to the unfed colonic fermentation. Results are shown for Experiment 1, Experiment 2 and Experiment 3 independently. Bars represent mean ± SD of biological replicates within each experiment. Insulin secretion is expressed as ng/10^6 cells·h.

3.4. Butyric and propionic acid concentrations in colonic fermentation supernatants positively correlate with insulin secretion

Potential relationships between fermentate composition variables, organic acids concentrations in colonic fermentate supernatants, and insulin secretion in EndoC-βH1 cells, were evaluated statistically and integrated into a unified framework using a Pearson correlation analysis (Fig. 5A). Butyric and propionic acid concentrations showed a significant positive correlation with insulin secretion ($r = 0.75$, $p < 0.001$ and $r = 0.64$, $p = 0.001$, respectively), suggesting that fermentates producing higher concentrations of these organic acids in the colonic fermentation supernatant might elicit greater insulinotropic responses. Conversely, formic acid ($r = -0.76$, $p < 0.001$) and lactic acid ($r = -0.73$, $p < 0.001$) were negatively correlated with insulin secretion. Butyric and propionic acid concentrations were strongly intercorrelated ($r = 0.87$, $p < 0.001$), consistent with their production during colonic fermentation. Additionally, a strong negative correlation was observed between protein and lactose content ($r = -0.98$, $p < 0.001$), reflecting the compositional differences between the dairy fermentates used.

To further support the insulinotropic potential of the identified organic acids, EndoC-βH1 cells were incubated with pure butyric acid or propionic acid at increasing concentrations (Fig. 5B). Butyric acid showed a non-linear dose-dependent response, with peak insulin secretion observed at 25 mM, followed by a decline at 100 mM, suggesting a potential inhibitory effect at supraphysiological concentrations (Tan et al., 2014). Propionic acid induced a progressive concentration-dependent increase in insulin secretion up to 100 mM. Together, these results support direct mechanistic evidence that butyric and propionic acid can stimulate insulin secretion in pancreatic β-cells, supporting their role as key bioactive components in the insulinotropic responses observed with the dairy fermentate colonic fermentation supernatants.

3.5. Colonic fermentation supernatants induce distinct dynamic insulin secretion profiles in murine pancreatic islets

Based on their distinctive profiles in the static experiments, the insulinotropic effects of the colonic supernatants generated following supplementation with three of the dairy fermentates (CFS1, CFS4 and CFS6 at 5% *w/v*) were tested using a dynamic model involving pancreatic islets. Insulin secretion was measured by dynamic perfusion over 30 min in murine islets. All groups were analysed with $n = 3$ independent islet preparations. The experimental protocol comprised four sequential phases: a basal 0 mM glucose period ($t = 0$–5 min), colonic supernatant treatment ($t = 5$–15 min), a 0 mM glucose washout ($t = 15$–20 min), and a 20 mM glucose stimulus ($t = 20$–30 min) (Fig. 6A). The colonic-phase insulin secretory response was quantified by AUC ($t = 6$–16 min) and normalised to the 20 mM glucose AUC from the same replicate to account for inter-preparation variability in islet secretory capacity.

When mice islets were exposed to flow, their insulin secretion patterns showed different behaviours (Fig. 6A). CFS 1 supernatant induced a modest increase in insulin secretion during the stimulation phase, rising from basal levels (~4 μg/ml) to ~6 μg/ml, with a small delayed peak during the 20 mM glucose phase (~8 μg/ml). On the other hand, CFS 4, induced a greater and sustained increase in insulin secretion than CFS 1 and 6 during the treatment phase, reaching a plateau near 10 μg/ml that persisted throughout the exposure period. Finally, CFS 6 induced a smaller insulin response, with a similar profile to CFS 1 with insulin levels raising at the glucose challenge phase. Raw AUC values were 47.98 ± 2.86, 79.43 ± 18.56 and 36.71 ± 9.18 μg/ml · min for CFS 1, CFS 4 and CFS 6 respectively. One-way ANOVA revealed a significant difference between groups ($F(2,6) = 10.105$, $p = 0.012$). Post-hoc Tukey HSD analysis indicated that CFS 4 induced a significantly greater insulin secretory response than both CFS 1 ($p = 0.043$) and CFS 6 ($p = 0.012$), while CFS 1 and CFS 6 did not differ significantly from each other ($p =$

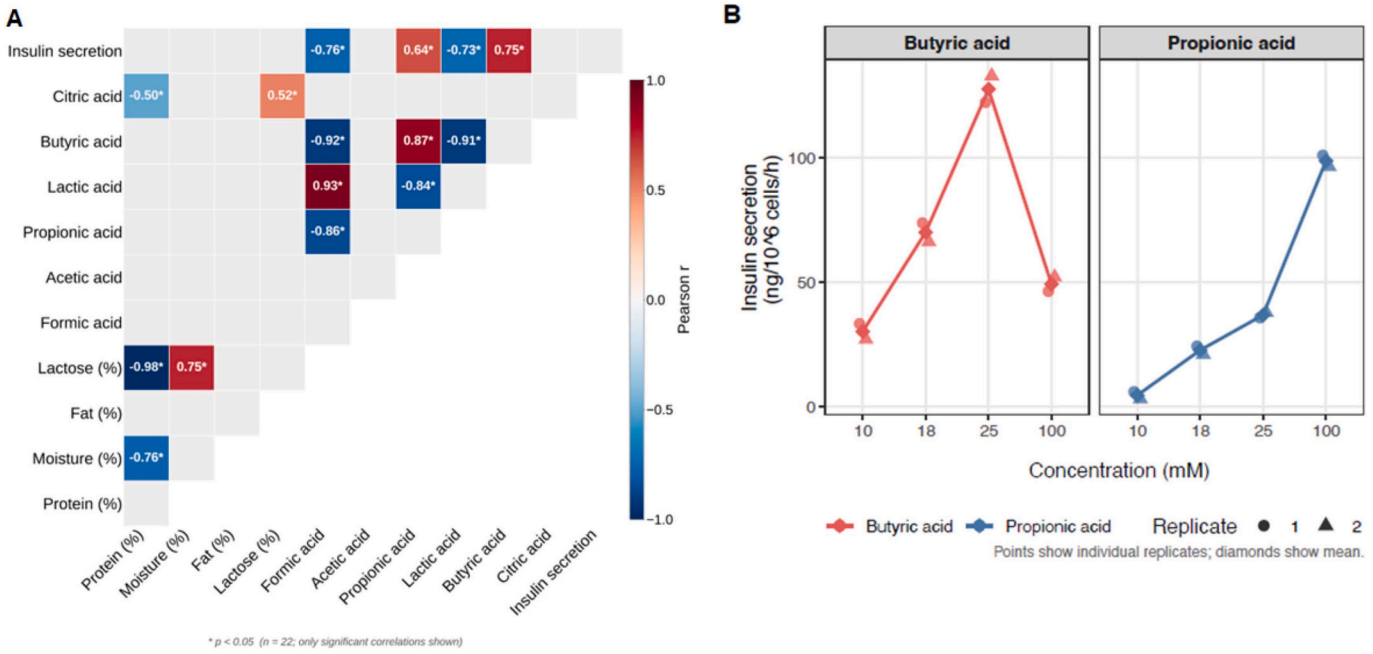


Fig. 5. Correlation between dairy fermentate composition and insulin secretion in EndoC-βH1 cells, and dose-dependent insulinotropic effect of propionic and butyric acids. (A) Pearson correlation matrix showing pairwise correlations between fermentate compositional variables (protein, moisture, fat and lactose content, expressed as %), organic acid concentrations measured in colonic fermentation supernatants (formic, acetic, propionic, lactic, butyric and citric acid, expressed in mM), and mean insulin secretion averaged across three independent experiments in EndoC-βH1 cells. Only statistically significant correlations are shown ($p < 0.05$, $n = 22$); non-significant pairs are shown in grey. Colour intensity reflects the strength and direction of the Pearson correlation coefficient (red = positive, blue = negative). (B) Dose-dependent insulin secretion in EndoC-βH1 cells following incubation with pure butyric acid (red) or propionic acid (blue) at concentrations of 10, 18, 25 and 100 mM. Individual replicates are shown as circles (replicate 1) and triangles (replicate 2); diamonds indicate the mean. (For interpretation of the references to colour in this figure legend, the reader is referred to the web version of this article).

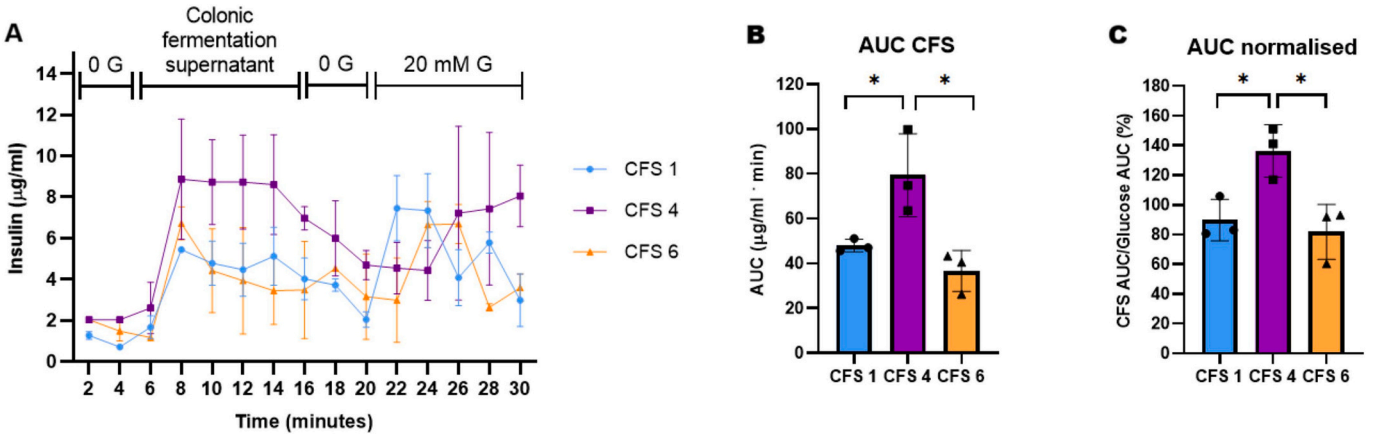


Fig. 6. Insulin secretory response of pancreatic islets to colonic fermentation supernatants (CFS) derived from INFOGEST-digested dairy fermentates. (A) Dynamic insulin secretion profile during perfusion. Islets were sequentially perfused with 0 mM glucose (5 min), colonic fermentation supernatant (CFS 1, CFS 4, or CFS 6; 10 min), 0 mM glucose (5 min), and 20 mM glucose (10 min). Data are expressed as mean ± SEM, $n = 3$ independent islet preparations. (B) Area under the curve (AUC) of insulin secretion during the CFS treatment phase ($t = 6$–16 min), calculated using the trapezoidal rule. (C) CFS-phase AUC normalised to the 20 mM glucose AUC from the same preparation, expressed as a percentage, to account for inter-preparation variability in islet secretory capacity. In B and C, bars represent mean ± SD with individual data points shown. Statistical comparisons were performed by one-way ANOVA followed by Tukey's post-hoc test. * $p < 0.05$.

0.525).

When normalised for potential variability in islet secretory capacity between independent preparations, the 20 mM glucose AUC did not differ significantly between groups ($F(2,6) = 0.927$, $p = 0.446$), confirming that islet preparations were comparable in secretory capacity across the three experimental groups. Following normalisation, the mean colonic fermentate supernatant-phase AUC expressed as a percentage of the glucose response was 89.8 ± 13.9% for CFS 1, 136.3 ± 17.5% for CFS 4, and 81.8 ± 18.5% for CFS 6. One-way ANOVA revealed a significant difference between groups ($F(2,6) = 9.265$, $p = 0.015$). Post-hoc Tukey HSD analysis indicated that CFS 4 induced a significantly greater insulin secretory response than both CFS 1 ($p = 0.033$) and CFS 6 ($p = 0.017$), while CFS 1 and CFS 6 did not differ significantly from each other ($p = 0.832$). These findings were confirmed by Kruskal–Wallis non-parametric analysis ($H = 5.422$, $p = 0.027$ for the non-normalised AUC; $H = 7.200$, $p = 0.027$). Overall, these results indicate that CFS 4 exerts a significantly stronger insulinotropic effect during the treatment phase than either CFS 1 or CFS 6, an effect that is independent of basal islet secretory capacity.

4. Discussion

As the prevalence of DM rises becoming a public health problem, different strategies are investigated to ameliorate and regulate its consequences. One such strategy focuses on the modulation of the gut microbiota and represents a reasonably accessible approach via dietary intervention (Garcia-Gutierrez et al., 2024). Fermented foods, including fermentates, are increasingly regaining attention as functional foods that provide health benefits, and their potential antidiabetic applications have started to be studied (Sivamaruthi et al., 2018). However, there is a lack of standardised methodology to screen these potential beneficial antidiabetic properties. Here, we propose a pipeline to characterise insulinotropic properties of fermentates and shortlist the most suitable to be further studied.

Fermentates modulate gut microbiota by providing specific substrates and metabolites that can favour the growth of bacterial groups associated with beneficial health outcomes. It has been reported that some fermentates and fermented foods showing beneficial outcomes are associated with higher Bacillota/Bacteroidota ratio due to the increase of fibre-fermenting bacteria in the gut microbiota composition (Dimidi et al., 2019; Marco et al., 2017; Stojanov et al., 2020). Moreover, the consumption of fermentates and fermented foods has also been associated with higher alpha-diversity (Leeuwendaal et al., 2022). The alpha-diversity, a measurement of the different species composition in a given ecosystem, of the gut microbiota has been connected with higher resilience to stressors and it is considered a measure of balance, meaning that higher alpha-diversity levels has regularly been associated with greater health (Manor et al., 2020), while lower values have been observed in instances of certain gut and systemic conditions (Li et al., 2022).

Our results show the presence of high relative abundances of *E. coli*, which has been previously reported and associated to the availability of certain metabolites during ex vivo distal colon studies (Mathur, 2023; Mukherjee et al., 2025). The presence of these abundances of *E. coli* could be explained by their fast growth using the available nutrients, constituting an initial bloom in contrast with the slower growth of other microorganisms present in the faecal samples.

The fact that the metataxonomic profiles at 1% concentration of the fermentates display a very similar profile to the unfed 24 h control shows that these levels of fermentate concentration do not have significant effects over the faecal microbiota composition. However, at 5% concentration, the dairy fermentate supplementation could be associated with an increase of bacterial taxonomic groups that have been linked with positive health outcomes in the past and have a slower grow than *E. coli*, such as *Bifidobacterium* sp., *Lactobacillus* sp. or *Blautia* sp. (Liu et al., 2021; Toscano et al., 2017). More specifically, these groups, beyond taxonomical ecosystem dynamics, are involved in the production of bacterial metabolites that have regulatory effects on the human host homeostasis (Brzozowski et al., 2009; Toscano et al., 2017; Wang et al., 2018). The observed differences in alpha diversity across fermentates at 5% concentration further highlight the role of substrate composition in shaping microbial community structure. Fermentate 5, with the highest protein content (90%), near-absent lactose (<0.5%) and the lowest fat content (0.5%), consistently showed the lowest species richness, Shannon entropy and Pielou evenness at 5% concentration. This carbohydrate-depleted profile would limit the availability of fermentable substrates for key saccharolytic species such as *Ruminococcus bromii* and *Bifidobacterium* species, which showed lower relative abundances under Fermentate 5 conditions relative to other fermentates at the same concentration, suggesting that macronutrient composition can directly modulate the selective pressure exerted on the gut microbial community with implications for downstream metabolite profiles.

One of the mechanisms by which the gut microbiota is linked to local and systemic effects impacting health is by the production of organic

acids, including SCFA. SCFA are produced by colonic fermentation and are involved in complex processes ranging from maintenance of the gut barrier integrity to neurologic conditions (Silva et al., 2020; Tan et al., 2014). They participate in the regulation of metabolism and inflammation by being major players in immune homeostasis and displaying antimicrobial, antitumorigenic and anti-inflammatory effects (Morrison and Preston, 2016; Yao et al., 2022). Pancreatic function is also affected by a number of molecules of gut microbiota origin, including SCFA (Ørgaard et al., 2019). More specifically, butyric acid has been shown to improve glucose homeostasis by ultimately stimulating insulin secretion via GLP-1 and PYY production (Jiao et al., 2020; Traisaeng et al., 2020). Butyric acid is also involved in other aspects of systemic glucose homeostasis beyond insulin secretion, by improving insulin sensitivity, increasing energy expenditure and reducing adiposity, in combination with propionic acid (Gao et al., 2009; Heimann et al., 2015). Propionic acid has been reported to have a direct effect stimulating human β-cell production of insulin and generally improving β-cell function in vitro (Pingitore et al., 2017). On the other hand, formate and lactate have been associated with different pathologies and inflammatory processes in the gut and beyond and lower levels are potentially desirable (Manosalva et al., 2021; Meiser et al., 2018; Pucino et al., 2019; Ternes et al., 2022).

Our results showed a positive correlation between butyric and propionic acid concentrations with an increase of insulin secretion in β-cells. Given the absence of glucose in the samples, we could hypothesise that a potential previous screening strategy could be developed to model the concentration of these SCFA by fermentation with insulin secretion and pro- and anti-inflammatory potential to make an informed selection on the food samples to be further tested. However, other analyses should be incorporated into the system to detect other metabolites that could be altering or interfering between the two elements, such as stimulation of the GLUT receptor of β-cells by metabolised glucose in the form of pyruvate or other amino acids (Prentki et al., 2013).

Besides quantifying the static production of insulin, we aimed to characterise how this insulin was released over time, to investigate potential applications for food design. For this, we designed a microfluidics device to host pancreatic islets and expose them to a flow. This strategy is increasingly used for diabetes research for a variety of applications, including pharmacological screening, disease modelling and quality control of cell therapy (Yin et al., 2022). The pancreatic islets are exposed to a flow that replenish consumed metabolites and removes the products of the resulting metabolic processes. The two trends that can be observed, high insulin release stimulated by the colonic fermentation supernatant followed by low positive control release (20 mM glucose) and low release stimulated by the colonic supernatant followed by high positive control release could be explained by the exhaustion of insulin production present in the pancreatic β-cells (Fu et al., 2013).

The dynamic insulin secretion profiles of colonic supernatants supplemented with fermentates 1, 4 and 6 reflect distinct bioactive properties that seem consistent with their compositional and fermentation characteristics. CFS 1 triggered a modest increase in insulin levels during stimulation, likely driven by low-level SCFA concentration in combination with a moderate protein content. The preserved response to 20 mM glucose suggests that this fermentate does not impair β-cell function and may support mild metabolic activation. In contrast, CFS 4 induced a stronger and more sustained insulin response, reaching a clear plateau throughout the stimulation phase. This effect is consistent with its high protein and SCFA content, especially butyrate and propionate, and likely involves a combination of peptide and FFAR-mediated mechanisms (Morrison and Preston, 2016). However, the reduced response to glucose suggests that β-cell activity may be partially exhausted following stronger initial stimulation. This is consistent with partial depletion of the readily releasable insulin pool, a well-described phenomenon following strong secretion and stimulation of pancreatic islets (Pfeifer et al., 1981). While this does not necessarily indicate cytotoxicity or irreversible functional impairment, as the observed exhaustion is likely transient and consistent with normal physiological feedback mechanisms, it raises relevant questions regarding the metabolic safety of repeated or prolonged exposure to high-protein, high-SCFA fermentates above physiological concentrations. Future studies incorporating cell viability assays, extended stimulation protocols and transcriptomic analyses would help to distinguish between transient secretory exhaustion and more sustained functional impairment, and to identify the molecular mechanisms underlying this response. CFS 6, on the other hand, did not stimulate a strong insulin response, including during the final glucose phase, which might align with its low protein and SCFA content and a high proportion of undefined components, that, once fermented, may interfere with insulin secretion. Overall, these results show how different fermentation outcomes translate into distinct functional signatures and highlight the usefulness of dynamic secretion profiling to identify both beneficial and non-responsive fermentates. When considered alongside the compositional data, these functional differences appear consistent with the macronutrient profiles of the fermentates. Fermentates 3, 4 and 5, which have the highest protein and lowest lactose content, produced the highest concentrations of butyric and propionic acid during colonic fermentation and elicited the strongest insulinotropic responses in the static assay. In contrast, Fermentate 1, with the highest lactose content (30%) and moderate protein content (56%), showed a distinct SCFA profile characterised by lower butyric and propionic acid concentrations and a more modest insulin secretion response in the static assay. Of the three fermentates selected for dynamic profiling, CFS 4, which has the highest protein content and lowest lactose content among the three, induced the strongest and most sustained insulin secretion response, consistent with its higher butyric and propionic acid concentrations, while CFS 6 showed the least pronounced response, consistent with its distinct compositional profile and lower SCFA production. This could have implications for ingredient and food design that can be adjusted depending on whether the goal is to release insulin more slowly or to boost a faster release. More accurate characterisation could be derived from the use of sensors to measure secretion in real-time and couple it with gene expression levels and transcriptomics to identify the specific mechanisms by which the stimulation is taking place.

Despite these promising results, the study has limitations that should be acknowledged. The number of biological replicates for both the SCFA characterisation ($n = 2$) and the static insulin secretion assay ($n = 3$) is limited, which constrains the statistical power of the analyses and prevents definitive conclusions from being drawn and robust models to be built. Accordingly, the fermentation and metabolite data are presented descriptively and should be regarded as hypothesis-generating rather than confirmatory, and the ranking of fermentates reported here is intended to prioritise candidates for subsequent validation rather than to establish efficacy. The effect sizes and variance estimates reported in this study provide the basis required to formally power such confirmatory studies. Additionally, the faecal fermentation model, while representative of colonic conditions, can vary depending on the donor microbiota composition, which may influence SCFA production profiles and limit the generalisability of the findings. The use of a pooled faecal standard, while an established strategy to minimise inter-individual variability in standardised screening platforms, masks the microbiome heterogeneity that exists between individuals, which may influence SCFA production profiles and downstream insulinotropic responses. Future studies using individual donor samples would help to capture the range of responses that might be observed in a real-world dietary intervention context. We are also aware that the use of EndoC-βH1 cells, while providing a reproducible and accessible human β-cell model, does not fully recapitulate the complexity of primary human islets, including the multicellular architecture and paracrine signalling present in native tissue, but the use of mice islets helps to strengthen the approach. Indeed, there are current limitations due to accessibility and maintenance of human islets, which have a narrow functional window and are

arguably the limiting factor. For this reason, the use of mice islets remains an affordable approach, as their functionality is highly similar to human and can be easily correlated. Furthermore, this method could enormously reduce the use of experimental animals, as only two islets are needed to detect quantifiable insulin (MacDonald et al., 2011). Another limitation is that the current pipeline does not account for the bioavailability and stability of the fermentate-derived bioactive compounds under physiological conditions, nor for potential interactions with the intestinal epithelium prior to systemic absorption. The integration of an epithelial barrier model, such as a Caco-2 cell monolayer, as an intermediate step in future iterations of the pipeline would more closely replicate the physiological route of metabolite exposure to pancreatic tissue. Finally, the correlation between SCFA concentrations and insulin secretion, while biologically plausible, is associative, and the very specific molecular mechanisms underlying the observed insulinotropic effects have not been directly investigated in this study.

Altogether, we present here a promising tentative pipeline to screen the potential insulinotropic properties of different fermentates, but with capability to further upgrades and applications and extension to other foods.

5. Conclusions and future prospects

As the use of fermented foods, including fermentates, is being investigated as a way to tackle insulin resistance, new methods are required to assess their potential insulinotropic properties. A simple method to characterise the amount of insulin released and the pattern on its release could facilitate the screening of promising fermented foods and fermentates that could be shortlisted for food design, for in vivo studies or human trials, contributing to optimise resources and use of experimental animals and increasing the ratio of success of these studies. This strategy also shows great potential for further development via detection of insulin release in situ using sensors or studying gene expression to identify molecular mechanisms involved in β cell regulation. Further applications could involve the use of patient islets for development of personal nutritional plans and/or medicine. Moreover, combination of other organs-on-a-chip, like gut, liver, skeletal muscle and white adipose tissue, would provide a platform to study the most meaningful interactions underpinning food and diabetes mechanisms.

Human and biological material

This study included organ or tissue donors.

This study includes human biological material and consent was obtained by donors, or their next of kin or legal representatives, for use in this study and for publication of the article. The samples used in this research were not sourced from executed prisoners or prisoners of conscience.

Studies in Human

This study was performed in compliance with relevant laws, regulatory frameworks and guidelines where the research took place.

This study was approved by the Clinical Research Ethics Committee of the Cork Teaching Hospitals, UCC. (Approval No. ECM 4 (mm) 09/03/2021)

Animal subject

This study was conducted in accordance with the following guidelines for animal welfare and/or reporting: Spanish Royal Decree 1201/2005 and the European Community Council directive 2010/63/EU.

This study was approved by the ethical committee of Miguel Hernandez University.

(Approval No. UMH.DF.LME.01.20 and UMH.IDI.LME.240119).

CRediT authorship contribution statement

Enriqueta Garcia-Gutierrez: Writing – review & editing, Writing – original draft, Visualization, Project administration, Methodology, Investigation, Funding acquisition, Formal analysis, Data curation, Conceptualization. **Alise J. Ponsero:** Writing – review & editing, Writing – original draft, Visualization, Investigation, Formal analysis, Data curation. **Víctor Calero:** Writing – review & editing, Visualization, Methodology, Investigation. **Helen Slattery:** Investigation. **Catarina Gonçalves:** Writing – review & editing, Supervision. **Laura Marroquí:** Writing – review & editing, Validation, Supervision, Resources, Methodology, Investigation, Funding acquisition, Conceptualization. **Paul D. Cotter:** Writing – review & editing, Validation, Supervision, Resources, Project administration, Funding acquisition.

Informed consent and patient details

Written informed consent to take part in the study and to publish the article has been obtained from all participants or their legal representatives. The privacy rights of participants have been observed.

Ethics approval and consent to participate

The Clinical Research Ethics Committee of the Cork Teaching Hospitals, UCC, approved the study (ECM 4 (mm) 09/03/2021) and faecal samples from healthy donors without antibiotic treatment in the previous six months were collected after written consent.

Experimental procedures were performed according to the Spanish Royal Decree 1201/2005 and the European Community Council directive 2010/63/EU. The ethical committee of Miguel Hernandez University reviewed and approved the methods used herein (approvals ID: UMH.DF.LME.01.20 and UMH.IDI.LME.240119).

Funding

This work was supported by Enterprise Ireland and the European Union‘s Horizon 2020 research and innovation programme under the Marie Skłodowska-Curie grant agreement number 847402 awarded to EG-G. L.M. is funded by grants PID2020-117569RA-I00, PID2023-147823OB-I00, and CNS2022–135505 funded by MCIN/AEI/10.13039/501100011033 and by the European Union NextGenerationEU/PRTR. Research in PDC's group is funded through Science Foundation Ireland (SFI) under grant number SFI/12/RC/2273 (APC Microbiome Ireland), and SFI together with the Irish Department of Agriculture, Food and the Marine, SFI/16/RC/3835 (VistaMilk), by the Enterprise Ireland funded Food Health Ireland project and by the European Commission under the Horizon Europe program under grant numbers 101060218 (DOMINO) and 101084642 (Co-Diet).

Declaration of competing interest

The authors declare the following financial interests/personal relationships which may be considered as potential competing interests: Dairy fermentates were provided by Carbery Ltd.

Acknowledgments

The authors want to thank Dr. Atenea Pérez-Serna, María Luisa Navarro and Beatriz Bonmatí for laboratory assistance, Dr. Reinaldo S. Dos Santos, Dr. Ramya Balasubramanian and Dr. José Ángel Salas-Millán for laboratory discussions, Dr. Gaston Allendez and Dr. Fiona Crispie for sequencing assistance and Dr. A. Kate O'Mahony for laboratory discussions and ideas to build the story, analyses and generation of graphical abstract. Graphical abstract created in BioRender. O'Mahony, A. (2025) https://BioRender.com/e40b8by.

Appendix A. Supplementary data

Supplementary data to this article can be found online at https://doi.org/10.1016/j.foodres.2026.120207.

Data availability

Data is in repository for public access

References

Awwad, S. F., et al. (2022). Invited review: Potential effects of short-and long-term intake of fermented dairy products on prevention and control of type 2 diabetes mellitus. *Journal of Dairy Science, 105*(6), 4722–4733.

Blanco-Míguez, A., et al. (2023). Extending and improving metagenomic taxonomic profiling with uncharacterized species using MetaPhlAn 4. *Nature Biotechnology, 41*(11), 1633–1644.

Brodkorb, A., et al. (2019). INFOGEST static in vitro simulation of gastrointestinal food digestion. *Nature Protocols, 14*(4), 991–1014.

Brzozowski, B., Bednarski, W., & Dziuba, B. (2009). Functional properties of Lactobacillus acidophilus metabolites. *Journal of the Science of Food and Agriculture, 89*(14), 2467–2476.

Burke, R. M., et al. (2020). Rotavirus and type 1 diabetes-is there a connection? A synthesis of the evidence. *The Journal of Infectious Diseases, 222*(7), 1076–1083.

Chatterjee, S., Khunti, K., & Davies, M. J. (2017). Type 2 diabetes. *The Lancet, 389*(10085), 2239–2251.

Constantinides, B., Hunt, M., & Crook, D. W. (2023). Hostile: Accurate decontamination of microbial host sequences. *Bioinformatics, 39*(12).

Dal Canto, E., et al. (2020). Diabetes as a cardiovascular risk factor: An overview of global trends of macro and micro vascular complications. *European Journal of Preventive Cardiology, 26*(2_suppl), 25–32.

Dimidi, E., et al. (2019). Fermented foods: Definitions and characteristics, impact on the gut microbiota and effects on gastrointestinal health and disease. *Nutrients, 11*(8), Article 1806.

Fooks, L. J., & Gibson, G. R. (2003). Mixed culture fermentation studies on the effects of synbiotics on the human intestinal pathogens campylobacter jejuni and Escherichia coli. *Anaerobe, 9*(5), 231–242.

Fu, Z., Gilbert, E. R., & Liu, D. (2013). Regulation of insulin synthesis and secretion and pancreatic Beta-cell dysfunction in diabetes. *Current Diabetes Reviews, 9*(1), 25–53.

Gao, Z., et al. (2009). Butyrate improves insulin sensitivity and increases energy expenditure in mice. *Diabetes, 58*(7), 1509–1517.

Garcia-Gutierrez, E., et al. (2024). Gut microbial metabolic signatures in diabetes mellitus and potential preventive and therapeutic applications. *Gut Microbes, 16*(1), Article 2401654.

Heimann, E., Nyman, M., & Degerman, E. (2015). Propionic acid and butyric acid inhibit lipolysis and de novo lipogenesis and increase insulin-stimulated glucose uptake in primary rat adipocytes. *Adipocyte, 4*(2), 81–88.

Jiao, W., et al. (2020). Butyric acid normalizes hyperglycemia caused by the tacrolimus-induced gut microbiota. *American Journal of Transplantation, 20*(9), 2413–2424.

Katsarou, A., et al. (2017). Type 1 diabetes mellitus. *Nature Reviews. Disease Primers, 3*, Article 17016.

Knip, M., et al. (2005). Environmental triggers and determinants of type 1 diabetes. *Diabetes, 54*(suppl_2), S125–S136.

Krueger, F. J. B. I. (2015). *Trim galore!: A wrapper around Cutadapt and FastQC to consistently apply adapter and quality trimming to FastQ files, with extra functionality for RRBS data*.

La Reau, A. J., et al. (2023). Shallow shotgun sequencing reduces technical variation in microbiome analysis. *Scientific Reports, 13*(1), 7668.

Langmead, B., & Salzberg, S. L. (2012). Fast gapped-read alignment with bowtie 2. *Nature Methods, 9*(4), 357–359.

Le Floch, J. P., et al. (1990). Blood glucose area under the curve. Methodological aspects. *Diabetes Care, 13*(2), 172–175.

Leeuwendaal, N. K., et al. (2022). Fermented foods, health and the gut microbiome. *Nutrients, 14*(7).

Li, Z., et al. (2022). Differences in alpha diversity of gut microbiota in neurological diseases. *Frontiers in Neuroscience, 16*, Article 879318.

Lijuan, C., et al. (2023). Fecal microbiota transplantation ameliorates type 2 diabetes via metabolic remodeling of the gut microbiota in db/db mice. *BMJ Open Diabetes Research & Care, 11*(3), Article e003282.

Liu, X., et al. (2021). *Blautia*—A new functional genus with potential probiotic properties? *Gut Microbes, 13*(1), Article 1875796.

MacDonald, M. J., et al. (2011). Differences between human and rodent pancreatic islets: Low pyruvate carboxylase, atp citrate lyase, and pyruvate carboxylation and high glucose-stimulated acetoacetate in human pancreatic islets. *The Journal of Biological Chemistry, 286*(21), 18383–18396.

Magliano, D.J. and E.J.J.I.D.A.t.e.B.I.D.F. Boyko, IDF Diabetes Atlas 10th edition scientific committee. 2021. **35914061**.

Manor, O., et al. (2020). Health and disease markers correlate with gut microbiome composition across thousands of people. *Nature Communications, 11*(1), 5206.

Manosalva, C., et al. (2021). Role of lactate in inflammatory processes: Friend or foe. *Frontiers in Immunology, 12*, Article 808799.

Marco, M. L., et al. (2017). Health benefits of fermented foods: Microbiota and beyond. *Current Opinion in Biotechnology, 44*, 94–102.

Martinez, K. B., Leone, V., & Chang, E. B. (2017). Western diets, gut dysbiosis, and metabolic diseases: Are they linked? *Gut Microbes, 8*(2), 130–142.

Mathur, H., et al. (2023). Methods to mitigate Escherichia coli blooms in human ex vivo colon model experiments using the high throughput micro-matrix bioreactor fermentation system. *MethodsX, 6*(11), 102393.

McIntyre, H. D., et al. (2019). Gestational diabetes mellitus. *Nature Reviews. Disease Primers, 5*(1), Article 47.

Meiser, J., et al. (2018). Increased formate overflow is a hallmark of oxidative cancer. *Nature Communications, 9*(1), 1368.

Mirghani Dirar, A., & Doupis, J. (2017). Gestational diabetes from A to Z. *World Journal of Diabetes, 8*(12), 489–511.

Morrison, D. J., & Preston, T. (2016). Formation of short chain fatty acids by the gut microbiota and their impact on human metabolism. *Gut Microbes, 7*(3), 189–200.

Mukherjee, A., et al. (2025). OPTIMATRIX v2.0: Optimised protocol to mitigate microbial blooms in the micro-matrix bioreactor platform used as an ex vivo human distal colon model. *MethodsX, 14*, Article 103275.

Nadal, A., & Soria, B. (1997). Glucose metabolism regulates cytosolic Ca2+ in the pancreatic β-cell by three different mechanisms. *Physiology and Pathophysiology of the Islets of Langerhans*, 235–243.

Nekoua, M. P., Alidjinou, E. K., & Hober, D. (2022). Persistent coxsackievirus B infection and pathogenesis of type 1 diabetes mellitus. *Nature Reviews. Endocrinology, 18*(8), 503–516.

O'Donnell, M. M., et al. (2016). Preparation of a standardised faecal slurry for ex-vivo microbiota studies which reduces inter-individual donor bias. *Journal of Microbiological Methods, 129*, 109–116.

O'Hearn, M., et al. (2023). Incident type 2 diabetes attributable to suboptimal diet in 184 countries. *Nature Medicine, 29*(4), 982–995.

Ørgaard, A., Jepsen, S. L., & Holst, J. J. (2019). Short-chain fatty acids and regulation of pancreatic endocrine secretion in mice. *Islets, 11*(5), 103–111.

Pfeifer, M. A., et al. (1981). The regulation of glucose-induced insulin secretion by pre-stimulus glucose level and tolbutamide in normal man. *Diabetologia, 21*(3), 198–205.

Pingitore, A., et al. (2017). The diet-derived short chain fatty acid propionate improves beta-cell function in humans and stimulates insulin secretion from human islets in vitro. *Diabetes, Obesity & Metabolism, 19*(2), 257–265.

Prentki, M., Matschinsky, F. M., & Madiraju, S. M. (2013). Metabolic signaling in fuel-induced insulin secretion. *Cell Metabolism, 18*(2), 162–185.

Pucino, V., et al. (2019). Lactate buildup at the site of chronic inflammation promotes disease by inducing CD4(+) T cell metabolic rewiring. *Cell Metabolism, 30*(6), 1055–1074.e8.

Ravassard, P., et al. (2011). A genetically engineered human pancreatic β cell line exhibiting glucose-inducible insulin secretion. *The Journal of Clinical Investigation, 121*(9).

Silva, Y. P., Bernardi, A., & Frozza, R. L. (2020). The role of short-chain fatty acids from gut microbiota in gut-brain communication. *Front Endocrinol (Lausanne)., 11*, 25.

Sivamaruthi, B. S., et al. (2018). A Mini review on antidiabetic properties of fermented foods. *Nutrients, 10*(12).

Stojanov, S., Berlec, A., & Štrukelj, B. (2020). The influence of probiotics on the Firmicutes/Bacteroidetes ratio in the treatment of obesity and inflammatory bowel disease. *Microorganisms, 8*(11).

Sun, H., et al. (2022). IDF diabetes atlas: Global, regional and country-level diabetes prevalence estimates for 2021 and projections for 2045. *Diabetes Research and Clinical Practice, 183*, Article 109119.

Tai, N., Wong, F. S., & Wen, L. (2015). The role of gut microbiota in the development of type 1, type 2 diabetes mellitus and obesity. *Reviews in Endocrine & Metabolic Disorders, 16*(1), 55–65.

Tan, J., et al. (2014). The role of short-chain fatty acids in health and disease. *Advances in Immunology, 121*, 91–119.

Ternes, D., et al. (2022). The gut microbial metabolite formate exacerbates colorectal cancer progression. *Nature Metabolism, 4*(4), 458–475.

Toscano, M., et al. (2017). Effect of Lactobacillus rhamnosus HN001 and Bifidobacterium longum BB536 on the healthy gut microbiota composition at phyla and species level: A preliminary study. *World Journal of Gastroenterology, 23*(15), 2696.

Traisaeng, S., et al. (2020). Leuconostoc mesenteroides fermentation produces butyric acid and mediates Ffar2 to regulate blood glucose and insulin in type 1 diabetic mice. *Scientific Reports, 10*(1), 7928.

Wang, M., et al. (2018). Beneficial changes of gut microbiota and metabolism in weaned rats with Lactobacillus acidophilus NCFM and Bifidobacterium lactis bi-07 supplementation. *Journal of Functional Foods, 48*, 252–265.

Yao, Y., et al. (2022). The role of short-chain fatty acids in immunity, inflammation and metabolism. *Critical Reviews in Food Science and Nutrition, 62*(1), 1–12.

Ye, J., et al. (2024). Phage cocktail alleviated type 2 diabetes by reshaping gut microbiota and decreasing proinflammatory cytokines. *Applied Microbiology and Biotechnology, 108*(1), 9.

Yin, J., et al. (2022). Pancreatic islet organoids-on-a-chip: How far have we gone? *J Nanobiotechnology, 20*(1), 308.